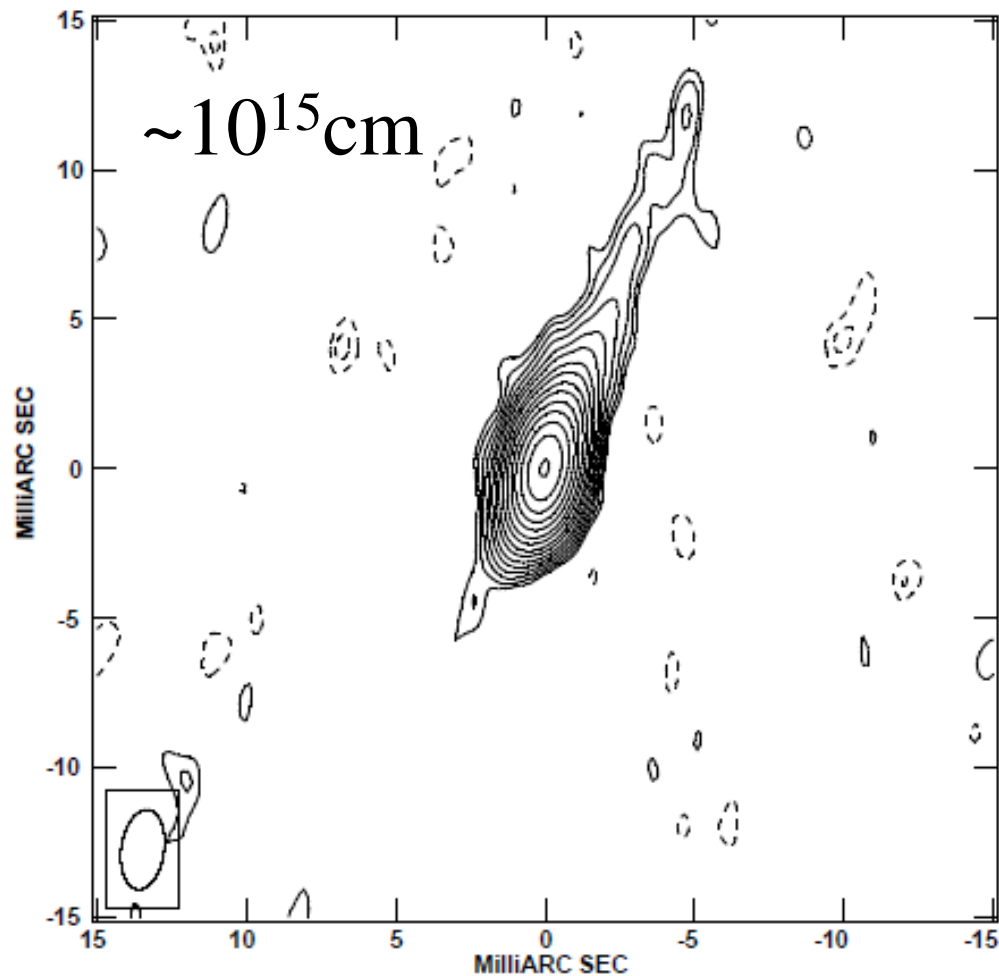


My work in 2023

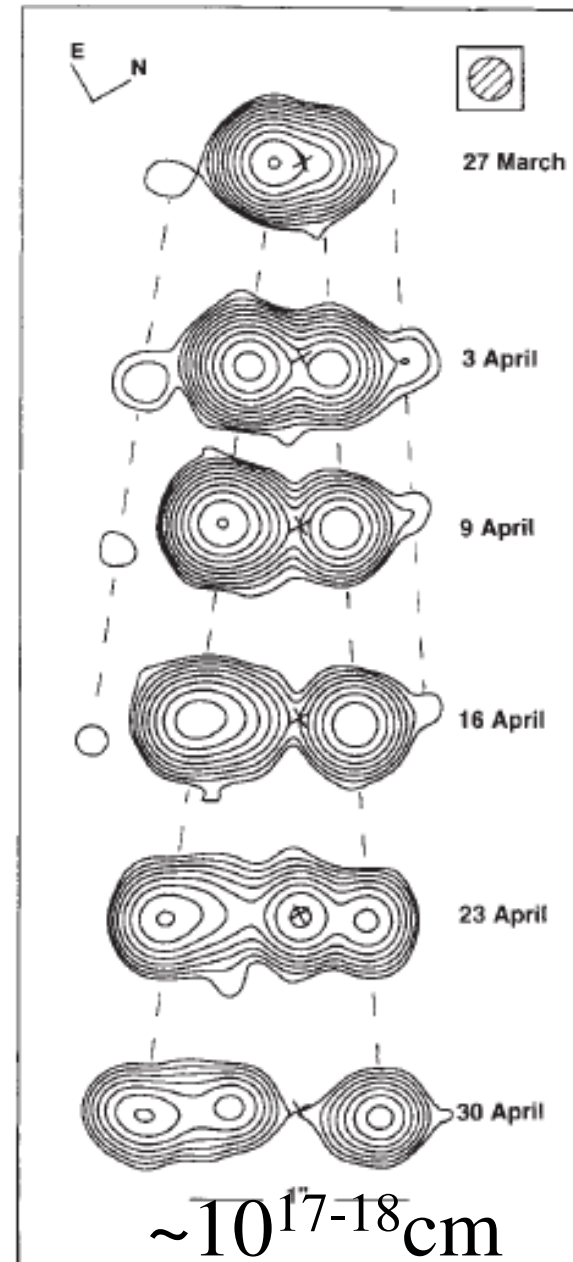
- 5 published individual papers.
- The nature of transient jets in accreting black-hole binaries: the jet power satisfies physical limits; surrounding low-density cavities can be filled with relativistic plasma.
- The jet in Cyg X-1 is likely to be misaligned w/r to the binary axis.
- The spins of black holes in accreting binaries are lower than previously thought.

Two very different kinds of jets in BH XRBs

Steady and compact in the hard spectral state



Cyg X-1, Stirling+ 2001, Rushton+ 2010

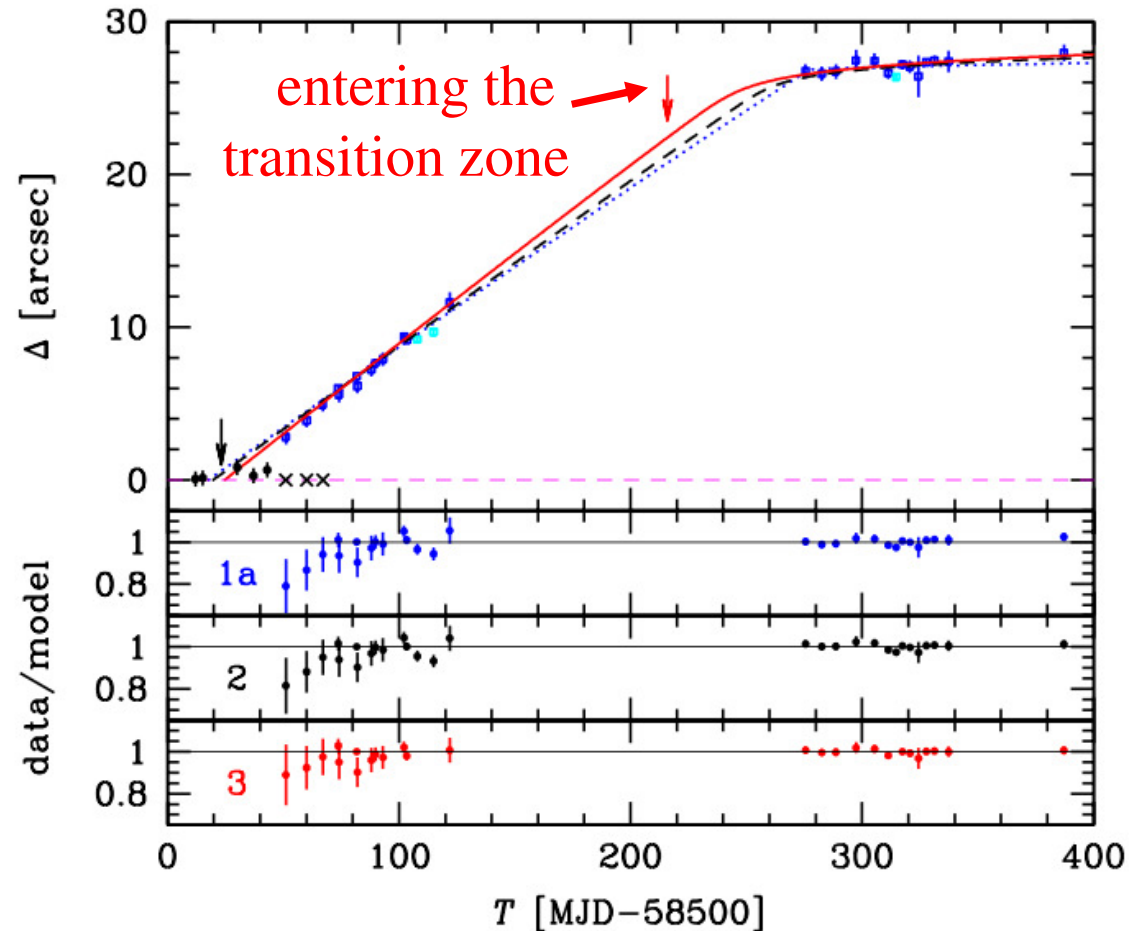
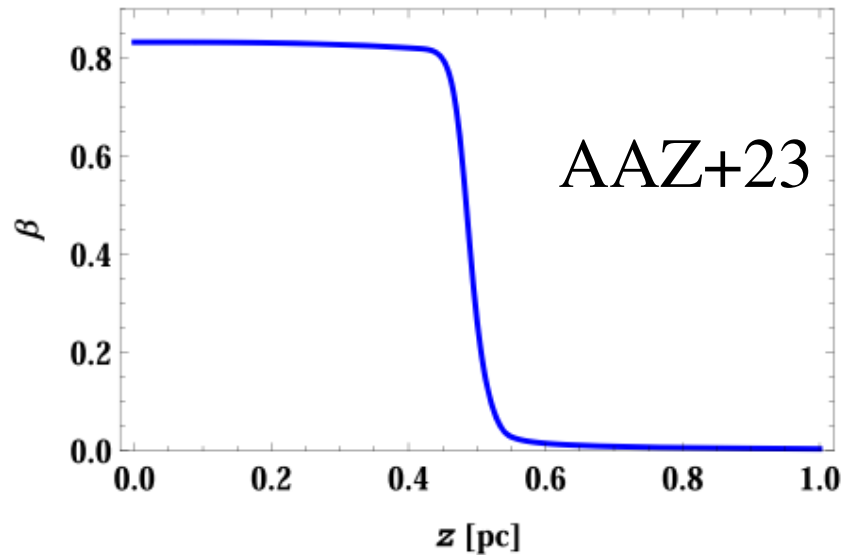


Transient jets at hard-to-soft state transitions

Mirabel+94

GRS 1915+105

Transient jets: a smooth transition zone between the cavity and the ISM solves the problem of extremely high jet power claimed earlier



The ejection slows down *entirely* in the transition zone. **The kinetic energy** at the MAD limit, $\approx 3 \times 10^{44}$ erg. The initial Lorentz factor $\Gamma_0 \approx 1.8$, the initial mass $\sim 4 \times 10^{23}$ g \rightarrow too heavy for e^\pm pairs.

Model dependence of the spin in LMC X-1

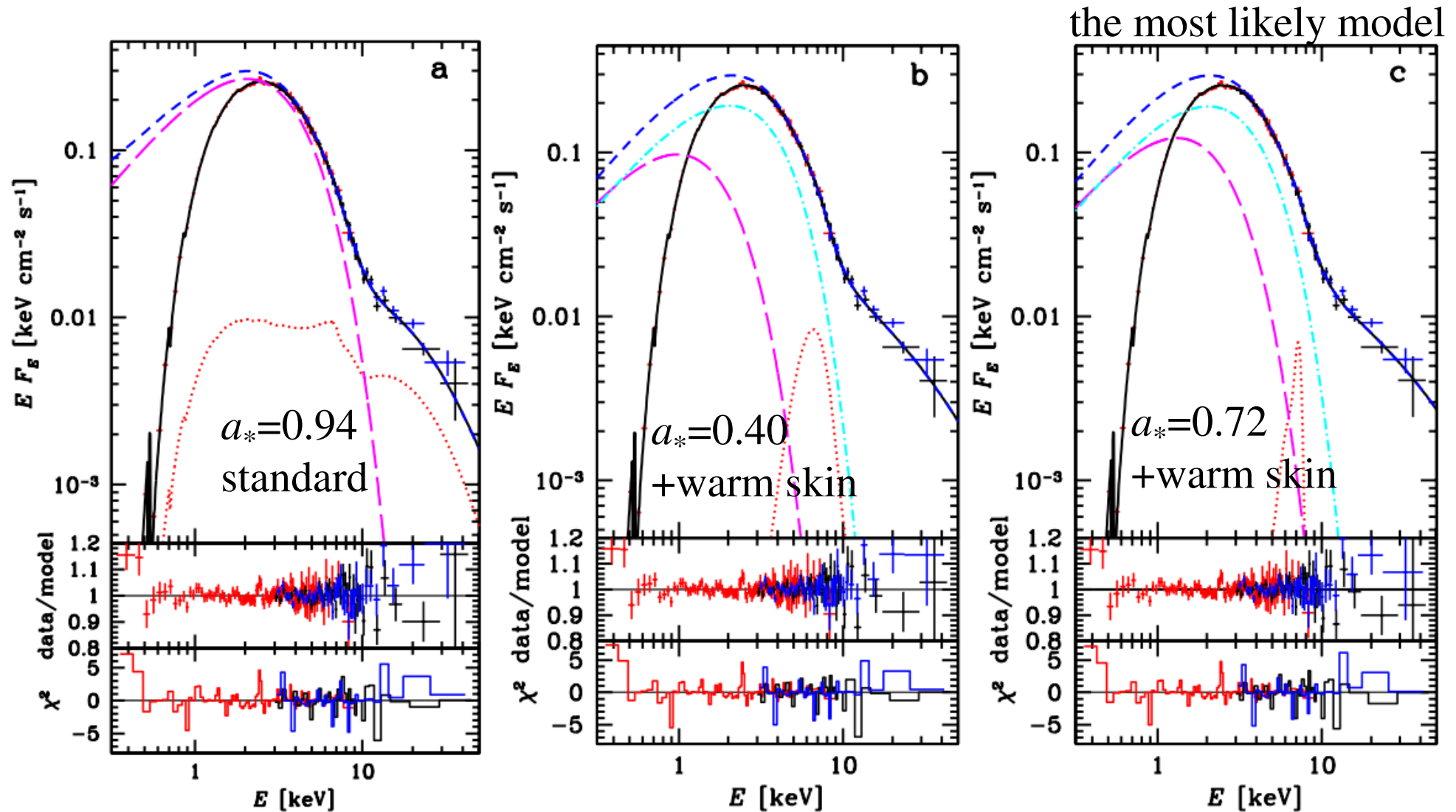
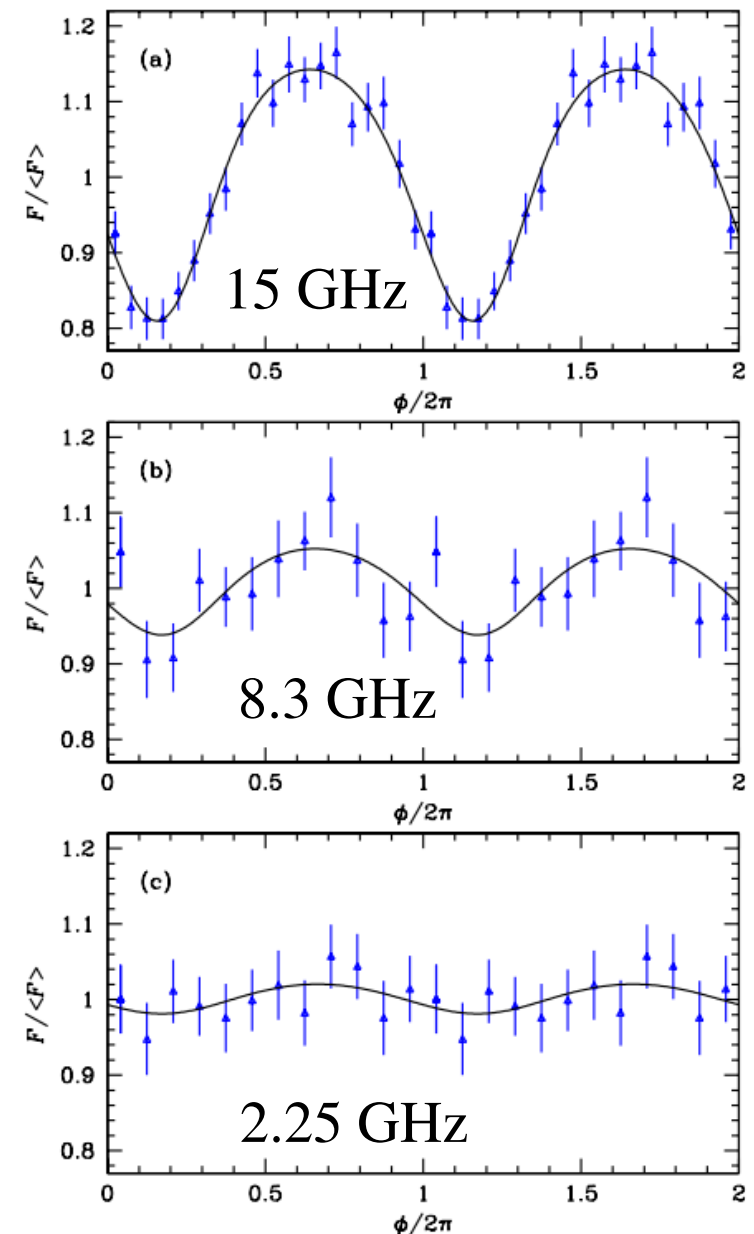


Figure 3. The NICER (red) and *NuSTAR* (black and blue) unfolded spectra, data-to-model ratios, and χ^2 contributions for (a) Model 2, $a_* = 0.94$; (b) Model 4, $a_* = 0.40$; (c) model 5, $a_* = 0.72$. The spectra are normalized to *NuSTAR* A. The total model spectra are shown by black solid lines, the reflection components are plotted by red dotted curves, and the unabsorbed models are shown by the blue short-dash curves. The magenta long dashes show the disk components before Comptonization, and the cyan dot-dashed curves in (b) and (c) show the disk component after Comptonization in the disk skin.

Fits to radio data give a solution to the geometry of Cyg X-1: the jet is not vertical and aligned with the binary axis

The modulation depth decreases with the decreasing ν and the offset of the minimum increases, implying emission at increasing distances from the black hole along the jet.

a = binary separation, f = wind scaling factor



h_{15}/a	f	$i(^{\circ})$	$\theta_{\text{BH}}(^{\circ})$	$\phi_{\text{BH}}(^{\circ})$	$\frac{\langle F_{\text{intr},15} \rangle}{\langle F_{15} \rangle}$	$\frac{h_8}{h_{15}}$	$\frac{\langle F_{\text{intr},8} \rangle}{\langle F_8 \rangle}$	$\frac{h_2}{h_{15}}$	$\frac{\langle F_{\text{intr},2} \rangle}{\langle F_2 \rangle}$
$2.6^{+1.4}_{-1.6}$	$0.7^{+0.3}_{-0.4}$	$27.5f$	19^{+12}_{-7}	73^{+21}_{-11}	$1.29^{+0.16}_{-0.09}$	$1.9^{+10.9}_{-0.3}$	$1.12^{+0.13}_{-0.12}$	$9.3^{+9.4}_{-5.2}$	$1.02^{+0.16}_{-0.02}$